Thermal activation of persulfates for wastewater depollution on pilot scale solar equipment

C. Telegang Chekem, S. Chiron, J.M. Mancaux, G. Plantard, V. Goetz

Thermal Activation of persulfates for wastewater depollution on pilot scale solar equipment

Telegang Chekem C[1,2], Chiron S.[1], Mancaux J[2,3]. M.; Plantard G.[2,3] and Goetz V.[2,*]

(1) UMR HydroSciences 5569, IRD, Montpellier University, 15 Avenue Ch. Flahault, 34093 Montpellier cedex 5, France;

(2) PROMES-CNRS UPR 8521, PROcess Material and Solar Energy, Rambla de la Thermodynamique 66100 Perpignan, France.

(3) UPVD, University of Perpignan Via Domitia, 52 Avenue Paul Alduy, 66100 Perpignan, France.

** Corresponding author: vincent.goetz@promes.cnrs.fr*

Abstract.

Thermal activation of new oxidant chemicals like Persulfate (PS) has recently gained attention in driving advanced oxidation processes (AOP) for a number of applications. ~~Persulfate (PS) is an oxidant chemical likely to undergo thermal activation to drive advanced oxidation processes (AOP) with respect to a number of applications.~~ On the other hand, addressing energy demand with carbon free and sustainable energy solutions represents an asset for new technologies in the modern society. This paper then investigates on the removal of pharmaceuticals residues in wastewater (WW), conducted with PS advanced oxidation reactions on a solar thermal pilot equipment. ~~I~~Indoor preliminary investigations on small scale laboratory experimentations shows how increasing temperature has a direct positive impact on pollutants degradations rate (k_{app} value ranging from $0.4 \cdot 10^{-3} s^{-1}$ at ambient to $10.4 \cdot 10^{-3}$ s^{-1} at 75°C)., However, after an experimental screening methodology, ~~carried out with a screening methodology, lead to~~ 65 °C and 200 µM appear as the appropriate target temperature and PS oxidant dosage to cope with both activation of PS oxidant and degradation of ten target micropollutants typically found in WW stream. Outdoor experimentations on the solar pilot equipment were ~~operated~~ conducted according to a batch running mode at a treatment capacity scale of a cubic meter. 95 % pollutant removal rate is achieved within 2 hours once the temperature has raised up to the target value (65 °C) in the bulk treated WW effluent. Series of treatment cycles under the natural day/night period demonstrate the reproducibility of the performance. As an early step result of the process optimization approach, heat recovery demonstration on the pilot equipment improves significantly the energetic balance over the now innovative thermal solar water treatment.

Keywords. Wastewater; -pollutant; persulfates; AOP; pilot; solar energy

Highlight

- Efficiency of ~~T~~thermal induced activation of persulfate ~~is effective~~ in removing biorefractory micropollutants in WW effluents.
- ~~Less than 2 hours needed to remove~~Up to 95% abatement of pollutants cocktail with 200 µM of persulfate and~~,~~ ~~under~~ 65 °C target temperature, on a solar pilot equipment. ~~and 200 µM of persulfate~~.
- ~~Degradation of ten target pollutants is achieved upon a solar pilot equipment running thermal activation of persulfate.~~
- ~~S~~Smart heat management system ~~system~~ to tackle solar energy intermittency.~~to improve the efficiency of the solar process with respect to energy balance.~~

Highlight graph

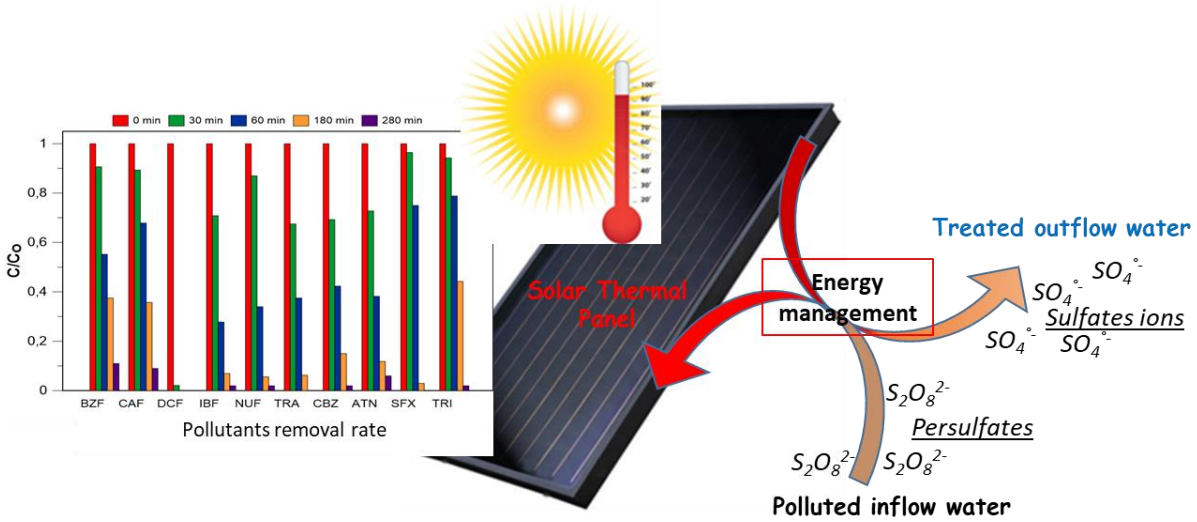

1. Introduction

Advanced oxidation processes (AOPs) are based upon the formation of highly reactive free radicals species from different routes. Owing to the high redox potentials, the way free radicals react and degrade soluble organics is highly relevant regarding environmental remediation (Brienza et al., 2016; Marjanovic et al., 2018; Shawaqfeh and Al Momani, 2010; Vilar et al., 2011). Typically, free radicals catalyzed chain reactions readily make possible degradation and/or mineralization of a wide range of hardly biodegradable organic molecules. Combined with the direct use of solar energy for radicals production, they offer a unique opportunity to design an oxidative treatment process, at almost no additional energy cost, in agreement with the concepts of green chemistry and sustainable development (Malato et al., 2016; Strazzabosco et al., 2019). For many years since the discovery of free radicals potential for water decontamination, hydroxyl radicals (OH°) have been considered as the most attractive (Brienza et al., 2014; Duran et al., 2010; Liu et al., 2018). In the late 1990s, OH° is successfully used to run *in situ* chemical oxidation reaction, based upon utilization of oxidant reactants such as ozone, potassium permanganate and hydrogen peroxide (Cai et al., 2018). Since then, sulfate radicals ($SO_4^{-\circ}$), generated from a primary oxidant such as persulfate (PS) ions ($S_2O_8^{2-}$) have also been progressively studied regarding major advantages such as the high redox potential (E^0 = 2.6 V/SHE) and the longer lifetime of corresponding sulfate free radicals, i.e. 1000 fold more than OH° radicals (Cai et al., 2018; Matzek and Carter, 2016). For any of these options, running the process with solar energy upon the well-known photo-Fenton (Fe^{2+}- H_2O_2, Fe^{2+}-- $S_2O_8^{2-}$), has been so far the most popular and sustainable way to achieve radicals production (Cuervo Lumbaque et al., 2019; Malato et al., 2016; Soriano-Molina et al., 2018). However, the acidic pH conditions required to avoid iron ions precipitation for achieving Fenton reaction, now appear as a serious bottleneck for process dissemination (Clarizia et al., 2017; Johnson et al., 2008).

A number of publications have then addressed on the possibility to run AOP_S under less acidic or mild pH conditions. In the event of using Fe^{2+} chelates under neutral pH conditions, the efficiency to achieve free radical chain reactions is still yet to be attractive (Clarizia et al., 2017; Ike et al., 2018; Matzek and Carter, 2016; Wu et al., 2014). Iron free direct generation of OH° from hydrogen peroxide has also been addressed very recently and seems promising, as far as solar driven AOPs are concerned (Aguas et al., 2019; Ferro et al., 2015). Regarding sulfate radicals ($SO_4^{-\circ}$), iron free heat activation route of persulfate (schematically represented with *Eq. 1*) is also reported (Cai et al., 2018; Ghauch et al., 2015; Olmez-Hanci et al., 2013) but few research studies addressed solar heat activation of PDS and the real ~~advantages~~ asset it could provide as a comparison with more conventional existing AOPs.

$$S_2O_8^{2-} + Heat \longrightarrow 2SO_4^{-\circ} \quad (1)$$

The few recent papers dealing with the issue showed how successful is the activation of persulfate (single used reactant) towards a wide range of biorefractory organic pollutants in water (Cai et al., 2018; Ghauch et al., 2012; Johnson et al., 2008; Yang et al., 2017). The results obtained on lab scale experiments are quite promising but the demonstration of the technique on real pilot equipment needs further investigation, especially in the case of solar irradiation used as the only source of energy. Indeed, regarding heat energy needed to achieve relevant target temperature, energy efficiency/profitability of what could be the future real processes is definitely relevant. Unlike conventional "in direct sunlight" photocatalysis scheme, thermal activation based process appears more "robust" with respect to heat energy collected (from sunlight) being stored over time for optimal usage, including during less fair weather episodes.

This paper investigates on the capacity of a pilot equipment to run solar driven heat activation of PS for water depollution. The system efficiency is investigated regarding emerging contaminants found downstream wastewater (WW) plants. To the best of the author knowledge, this is the first time a pilot scale solar demonstration is used to run PS thermal activation for the removal of micropollutant in real WW stream. In the south west of Europe, some areas face overexploitation of water resources together with lack of precipitations. In the perspective of achieving the new circular economic paradigm of water reuse, emerging and biorefractory microcontaminants need to be discarded from WW effluents. However, most of these microcontaminants are biorefractories molecules like pharmaceuticals and pesticides constituents, which are hardly removed by existing biological treatments (Devi et al., 2016; Faraldos and Bahamonde, 2017; Oh et al., 2016). At the meantime, the high toxicity level and bioaccumulation fate of a number of microcontaminants represent a real threat to public health and environmental protection as well (Brienza and Chiron, 2017; Miralles-Cuevas et al., 2018). The main objective of this study is to achieve PS thermal activation and then removal of emerging pollutants from WW, on a pilot scale newly designed solar equipment. Prior to real pilot scale demonstrations, degradation of ten target molecules was lab scale investigated on small wastewater samples. This was necessary to collect information on the influence of relevant experimental parameters on the depollution process. The ultimate aim was then to set favorable conditions for running the pilot equipment under solar irradiated and optimal basis.

2. Preliminary experiments

This section deals with indoor experiments, carried out in the laboratory prior to real solar pilot scale experimentations. Working first on low WW volumes (500 mL) was necessary to understand how impactful experimental parameters on degradation process are.

2.1. Wastewater and reagents

WW was used in this study to keep the pilot set up under “real life - like” experimental conditions. WW was collected downstream of a WW treatment plant in the south of France. Suspended materials were removed after an additional sand filtration and WW was stored for less than 2 days at 4 °C before usage. On Table 1 ~~presents~~ are the average values of some physicochemical parameters of WW samples.

Table 1. Physicochemical properties of wastewater samples

MES ($g.L^{-1}$)	pH (-)	Cond. ($\mu S.m^{-1}$)	TOC ($mg.L^{-1}$)	DCO ($mg.L^{-1}$)	NTK ($mg.L^{-1}$)	NGL ($mg.L^{-1}$)	SO_4^{2-} ($mg.L^{-1}$)
8.5	7.4	669	12.2	28.1	7	9.2	195

For depollution experiments, WW samples were spiked with a cocktail of ten target molecules (**Table 2**) at $\mu g.L^{-1}$ concentrations range. The molecules belong to different families of pharmaceuticals reportedly found in WW effluents in the south west of Europe (Brienza et al., 2016). They were obtained from *Sigma Aldrich* at more than 98% purities, together with potassium iodide (99.5%) and sodium bicarbonate (99,7%). Potassium persulfate (99%) was purchased from *Acros Organics*. All the chemicals were analytical reagent grade.

For liquid chromatography, the reagents used in this study were of ultra-pure HPLC grade.

Table 2. List of emerging contaminants used as target molecules

Family	Target Molecules
Nervous system stimulant	Caffeine (CAF)
Lipid-lowering agent	Bezafibrate (BZF)
Antihypertensives	Atenolol (ATN)
Anti inflammatory	Diclofenac (DCF)
	Ibuprofen (IBF)
	Niflumic acid (NUF)
	Tramadol (TRM)
Anticonvulsant lipid regulators	Carbamazepine (CBZ)
Antibiotics	Trimetoprim(TRI)
	Sulfamethoxazole (SFX)

2.2. Analytical Apparatus and measurement procedures

An ultra-high performance liquid chromatography - electrospray - orbitrap mass spectrometer (UHPLC-MS/MS) was used to determine the concentrations of contaminants in WW samples, under both positive and negative modes of the ion spray source. The UPLC compartment (*Agilent 1290 infinity*) is equipped with a C-18 analytical column under 0.2 $mL.min^{-1}$ flow rate of binary solvent mixture (water and acetonitrile). This was coupled to a MS/MS tandem 6460 triple quad mass spectrometer. The accuracy and sensitivity of the analysis system and then the corresponding protocol comply with the detection of pollutants at very low concentrations (down to ng/L concentrations range).

The residual persulfate concentration was determined according to a new spectrometric method recently detailed in the literature (Liang et al., 2008; Zhao et al., 2015). The method is straightforward and less time consuming as a comparison with the conventional well known iodometric dosage. A UV-vis spectrophotometer (VL-320 model) equipped with quartz cuvettes (1 cm beam path) was used to read the absorbance of solutions after reaction of PS with potassium iodide (KI). Calibration was carried out on a series of prepared standard solutions (20 mL) with PS concentration ranging from 0 to 10 mg/L while keeping constant KI and $NaHCO_3$ concentrations (respectively 1 and 0.1 g in 20 mL solutions, respectively). The water/KI/PS/ $NaHCO_3$ mixture was hand shaken and then allowed to react for about 30 min. The intensity of the resulting yellowish color depending on the amount of PS which reacted with the KI excess concentration. It's worth mentioning that $NaHCO_3$ is also added to prevent air oxidation of KI reactant (Liang et al., 2008). Absorbance reading was carried out at 400 nm after sample solutions have followed the same protocol of calibration standards except PS addition step. Dilution factors in the measurement solutions were considered for the determination of concentrations.

TOC measurements were performed with a TOC meter equipment (Shimadzu TOC-VCSH/CSN) after total and inorganic carbons have been determined.

2.3. Depollution experiments

For indoor lab scale experiments, contaminated WW samples contained in 500 mL flasks were prepared after proper dilution of corresponding reagents. For the 10 target molecules of this work, the concentration in the treated solutions was set at between 2.2 – 25 $\mu g.L^{-1}$, i.e. close to naturally occurring concentrations (Brienza et al., 2016). Suitable dilutions were carried out from a 2 mM PS mother solution to get final treated solutions of different oxidant concentrations (≤ 500 µM). Flasks containing the mixture were placed into a laboratory thermal water bath set at a given temperature. At proper time ~~interval~~frequency, 5 mL of samples were withdrawn for analytical measurements (target pollutants, PS and TOC) according to principles and procedures described in section 2.2. Kinetic profiles were then obtained at different initial PS

concentrations and temperatures. On a set of repeated experiments (triplicates), standards errors on quantification results were estimated lower than 6% (experimental reproducibility and instrumentation uncertainty).

2.4. Influence of experimental parameters on pollutants degradation

- Effect of temperature

Fig. 1 sets out with average concentrations kinetics profiles at different temperatures, considering ~~all~~ the ten target pollutants as whole ~~taken together~~. At room temperature (20 °C), pollutants degradation is almost negligible i.e. less than 8 % removed after 5 hours of reaction (overlapping with measurement accuracy threshold). Pollutants disappearance rate becomes significant as the temperature of the treated solution increases. This is in agreement with PS concentration profiles at different temperatures (Fig. 2). They suggest that thermal activation of persulfate for generation of free radical species is temperature dependent as reported in previous studies in the literature (Cai et al., 2018; Johnson et al., 2008).

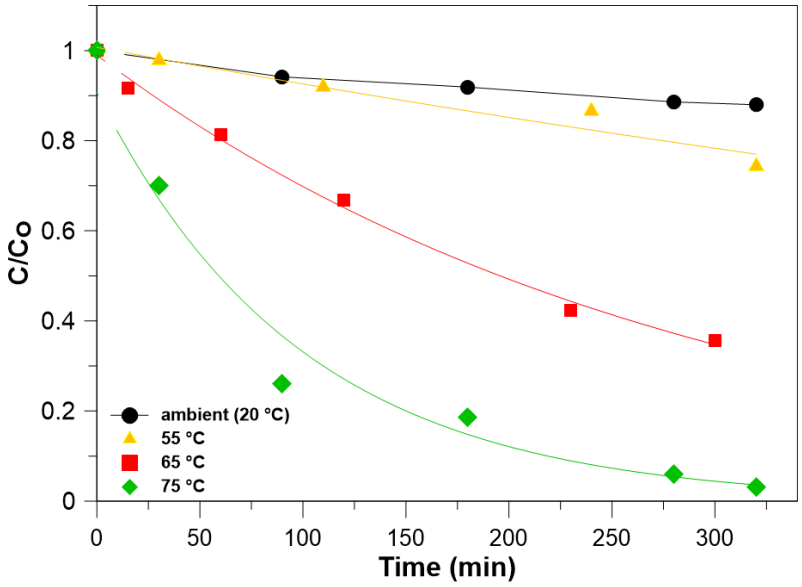

Fig. 1. Kinetic profiles of μ–pollutants removal (average concentration) at different temperatures (Initial PS concentration 200 μM, C_o average value= 5.2 μg.L^{-1})

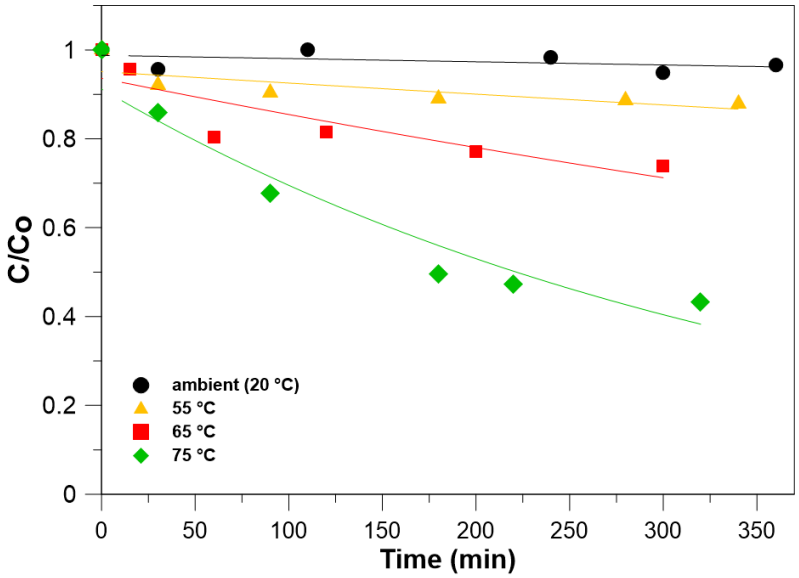

Fig. 2. Kinetic profiles of PDS oxidant disappearance at different temperatures (Initial PS concentration 200 µM)

Fig. 3 is the first order rate representation of kinetic profiles at different temperatures. One can see that the more the temperature applied, the higher the pseudo-first-order rate constant of pollutants disappearance kinetics. The exponential trend on the increase of k_{app} rate constant (from $0.4 \cdot 10^{-3}$ s^{-1} at 20 °C to 10^{-2} s^{-1} at 75 °C) is consistent with the fate of sulfate free radicals appearance under thermal activation conditions, reported in the literature (Deng et al., 2013; Johnson et al., 2008). Regarding PS thermal decomposition under different experimental conditions, Johnson *et al.* (Johnson et al., 2008) ~~showed~~ highlighted a pseudo first order profile ~~that~~ of PS~~persulfate~~ thermal activation ~~follows a pseudo first order profile~~. They also obtained an exponential increase of rate constant regarding sulfate ion production from PS within 30 – 70 °C temperature range. Considering the short lifetime of sulfate radicals ($SO_4^{-\circ}$), it is worth mentioning that degradation of pollutants is correlated to the capacity of the system to generate $SO_4^{-\circ}$ free radicals on a continuous basis. Activation energy has been calculated after setting a correlation (R^2 = 0.86) with respect to 1/T and then ln(k_{app}) according to Arrhenius equation,

$$Ln(kapp) = \ln A - E_a / R \cdot T \qquad 2$$

where *A* being the Arrhenius constant, E_a the activation energy (kJ.mol^{-1}), T the absolute temperature (K) and R the universal gas constant (8.314 J.mol^{-1}.K^{-1}). The linear regression obtained from experimental points is represented on Fig. 3 inserted panel.

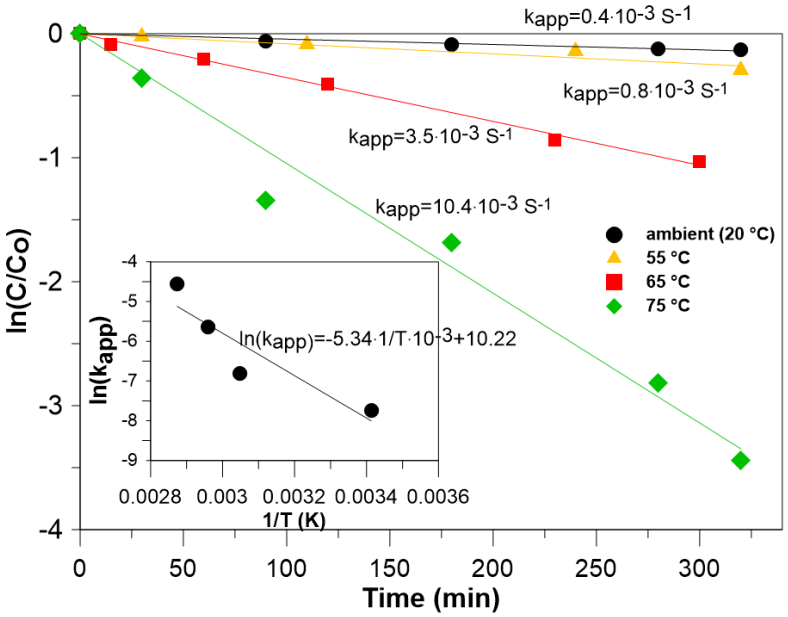

Fig. 3. First order representation of kinetic profiles of pollutants elimination at different temperatures (Initial PS concentration 200 µM, Co = 2.2 – 25 µg.L^{-1})

232

233 E_a calculated value obtained in this study, 44.39 kJ.mol^{-1}, is typically lower than what is found
234 in a number of papers in the literature (Deng et al., 2013; Ghauch et al., 2015; Ji et al., 2015;
235 Yang et al., 2017). Fan *et al.* (Fan et al., 2015) and Deng *et al.* (Deng et al., 2013) worked
236 respectively on Sulfamethoxazole and Carbamazepine and obtained E_a values above 100
237 kJ.mol^{-1}, suggesting more difficulties in degrading these molecules as compared to results in
238 this study. Actually, E_a value obtained at this stage is representative of the mean value of all
239 the individual behaviors of the ten target molecules of this study.

240 Profiles of Individual target molecules under 75°C treatment temperature are presented in Fig.
241 4. One can observe how molecules react differently to thermal treatment activation. Ibuprofen
242 and Diclofenac are totally removed after 60 mins of reaction. Molecules like Cafeine and
243 Tramadol need more than 2 hours for complete removal **(**Fig. 4.a). Nuflimic acid Bezafibrate
244 and Trimetoprim are among the most harsh with about 85 % of removal rate achieved after 5
245 hours of reaction. However, regardless the pollutant without oxidant, less than 20% removal
246 rate is attained under the same experimental conditions (Fig. 4.b), indicating a slight
247 thermolysis degradation of pollutants. Thermolysis contribution then stands for very little on
248 removal rate achieved under PS driven conditions.

249

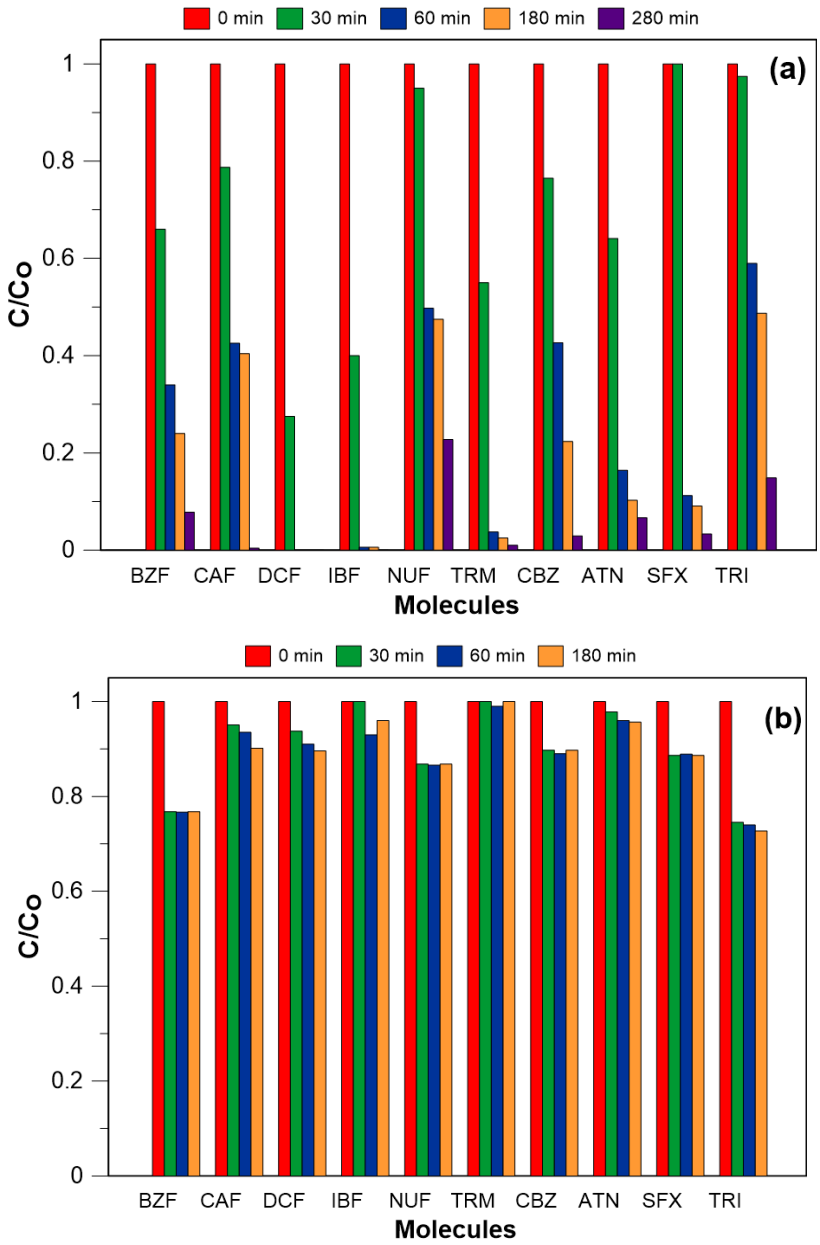

Fig. 4. Kinetic profiles of elimination of individual target molecules (a) with and (b) without oxidant. PS oxidant concentration 200 µM - Temperature 75 °C.

- Effect of oxidant concentration

Fig. 5 is a representation of the kinetics profiles of pollutant average concentration at four different concentrations of PDS oxidant (0, 100, 200 and 500 µM). 8% removal rate is hardly achieved after 5 hours reaction without PDS reactant, indicating a slight thermolysis of the target molecules. In the presence of oxidant, pollutant concentration is significantly decreased to evince the main role of oxidant activation regarding pollutants disappearance in the solution.

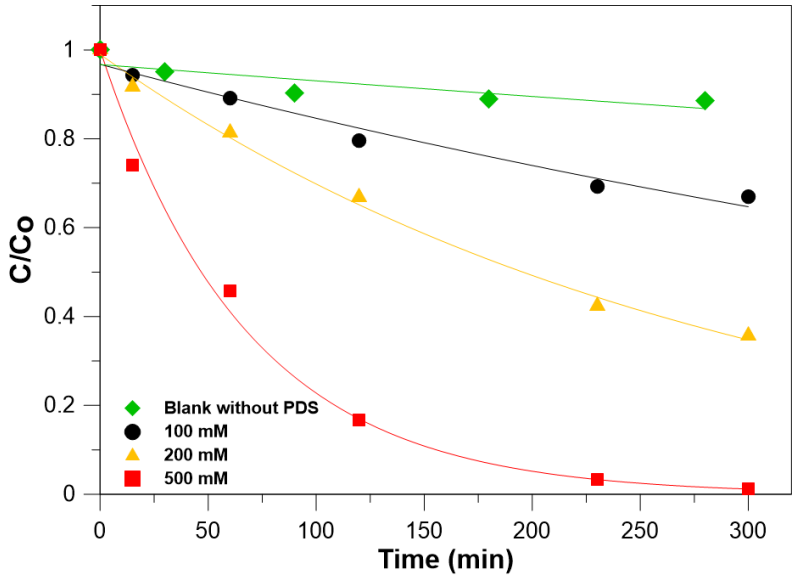

Fig. 5. Kinetic profiles of pollutant removal at different concentrations of PS oxidant - Temperature 65 °C.

The increase of pollutants removal rate with PS concentration is in agreement with papers in the literature (Cai et al., 2018; Marjanovic et al., 2018; Yang et al., 2017). Indeed, increasing oxidant concentration is favorable to organic removal as higher concentrations of sulfates radicals are available for oxidation. However, the utilization of PS reactants should take into account environmental norms and standards regarding release of sulfates in natural streams, some health disorders being reportedly associated to high level of sulfates in water. Few hundreds mg of sulfate ions are most often admitted in wastewater (Heizer et al., 1997). Later on in this paper, only 200 µM of PS oxidant will be considered. A maximum of 40 mg/L of sulfate ions is likely to be released out, should initial PS oxidant being completely converted.

- Comparison of the fate of coexisting chemical species

Fig. 6 is a comparison between kinetic breakthroughs of coexisting chemical species in the treated solution i.e. target pollutants, PS oxidant and organic charge represented by TOC. After 6 hours of reaction, less than 10 % of the gross initial TOC load (about 12.2 $mg.L^{-1}$) is removed. At the meantime, the target pollutants are completely discarded when 60 % of oxidant initially present has been consumed. This is a relevant example of the selective activity of sulfates free radicals towards target pollutants (in $\mu g.L^{-1}$ concentrations range).

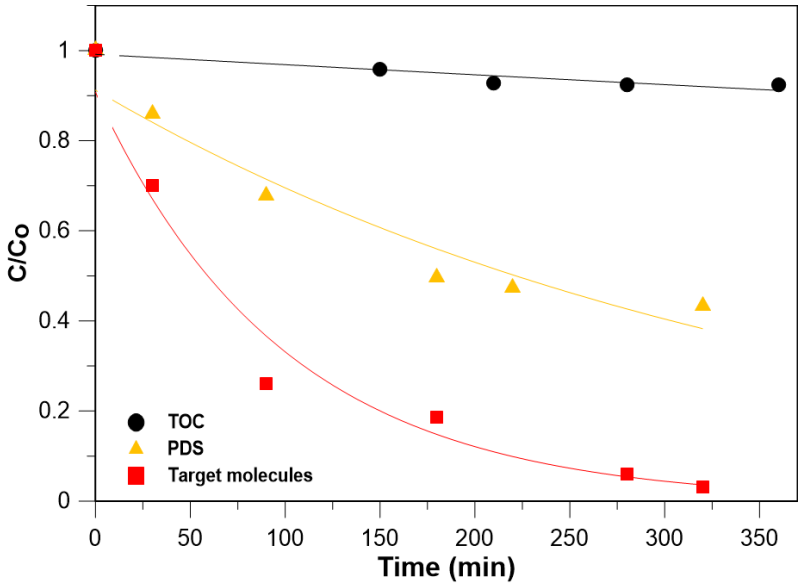

Fig. 6. Kinetic profiles of coexisting chemical species in treated solution. PS oxidant 200 µM, Temperature 75 °C.

Sulfate selectivity is already reported in a number of studies in the literature. Cai et al., 2018, achieved a complete degradation of 2.4-dichlorophenoxyacetic acid from contaminated WW with 65 % remaining TOC at the end of reaction. Working on winery wastewater, Amor *et al.* (Amor et al., 2019) obtained similar results but succeeded in removing total TOC after combining thermal and UVC/iron activation of persulfates. In their research work with Titania photocatalyst, Shawaqfeh and Al Momani (2010) needed two times longer period to achieve TOC load as compare to time needed for removing some typical micropollutants. In this study, after 5 hours of reaction, 60 % of initial PS concentration is being consumed. Assuming PS being completely consumed over degradation reactions, this accounts for about 20 mg.L^{-1} residual concentration, very low value regarding standards on WW effluents release (Heizer et al., 1997).

3. Pilot scale experiment

3.1. Pilot experimental set up

A picture of the pilot is presented in figure 7, together with a descriptive diagram. It is mainly composed of two tanks (upper and lower) of 1 m^3 capacity, three flat solar panels (3 x 2 m^2 light harnessing surface) set in series and a heat exchanger (plate type model). Irradiation conditions were monitored with a radiometer (Kimo CR-110) and temperatures of WW in the upper tank, at the outlet of the panels and the inlets/outlets of the heat exchanger were measured with thermocouples (*K type*) connected to a data acquisition system. For simulation of naturally occurring conditions, the inlet concentration of the ten target pollutants stood between 12 – 22 µg.L^{-1}.

Treatment consisted in two successive phases. First, heating of the WW effluent to a target temperature and then oxidation reactions conducted with PS reactant, introduced from a reagent vessel. For running the process, a volumetric pump ($Pump_{rec}$) allows WW recirculation over a closed fluid loop connecting the upper tank with the thermal receiver (solar heating panels). For optimization purposes regarding solar energy utilization, recirculation takes place only when WW temperature straight at the thermal receiver outlet is above a representative value in comparison to the temperature in the upper tank (ΔT threshold setting). The same regulation approach is used in traditional solar water heating system for preventing preheated effluent to undergo reverse cooling off under poor irradiation condition (cloudy periods & nights). Raising WW to 65°C was the target to achieve before injection of PS oxidant (solenoid dosage with *Verderdo VE1-C* pump). Periodically, few amounts of WW effluent were collected from the system for analysis.

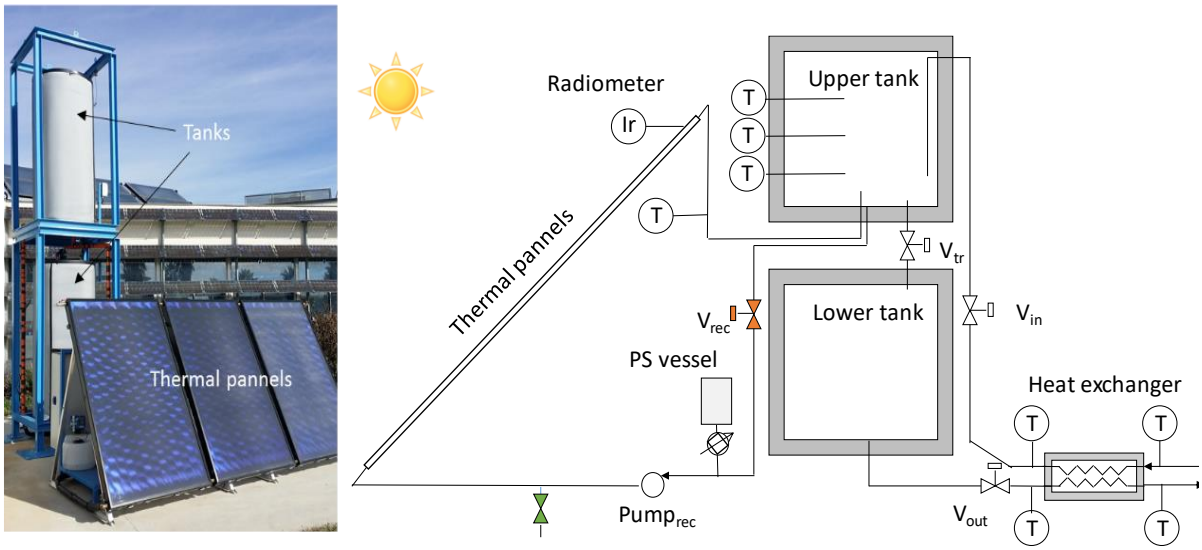

Fig. 7 Water treatment solar pilot picture and descriptive diagram

After completion of degradation, an integrated heat exchange system is used to transfer heat from the outflowing hot treated WW to a new contaminated WW volume entering the system. First, the treated WW effluent in the treatment tank (upper tank) is transferred to a lower tank. From the lower tank, treated WW effluent is cooled down before leaving the system and the energy released is used for heating new contaminated WW volume filling in the upper tank at the meantime. This “heat energy management system” is a reliable way to tackle the issue of energy saving and low investment on nominal surface area of thermal panel.

3.2. Wastewater depollution on solar pilot

Figure 8 shows the variation of WW temperature over six days in the row, on the month of June in Perpignan. The corresponding solar irradiation (W.m^2) is also presented. For better illustration and interpretation of results, night periods data have been removed as well as earlier time in the morning and later in the afternoon, i.e when irradiation is quite poor (looping pump off).

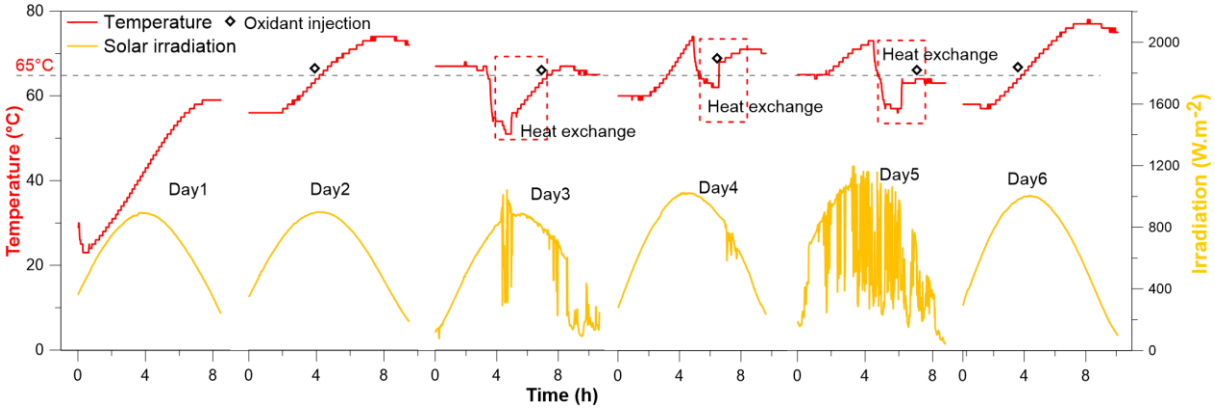

Fig 8. Effluent temperature and solar irradiation in 6 days in the row, heat and oxidant management between one batch treatment to another (800 L of WW effluent)

Higher solar irradiation was registered on day 1 and 2, typical to summer weather in this part of Europe, with a daily average of the incident radiation energy ranging around 6.8 kWh/m^2 (between 7 a.m. to 5 p.m.). Day 3 witnessed some cloudy episodes and day 5 was definitely cloudy, with significant decrease on radiation energy collected into heat form.

Day 1 starts first by filling the treatment tank with 800 L WW prior to data collection (Fig. 8). Starting from ambient temperature of WW (25 °C), a day of irradiation was not sufficient to achieve 65 °C threshold of WW temperature. At the end of the first day, the treated effluent caps at around 60°C and because of heat losses over the equipment during night window, a slight decrease (2-3 °C) is observed before solar heating resumed the second day (Fig. 8). Thereafter, 3 to 4 hours were needed to reach the expected 65°C. Theoretically, about 37 kWh$_{th}$ of thermal energy are expected for elevation of 800 L of WW from 25 to 65 °C. In practice, the required solar energy backing this temperature elevation is the amount of radiation received right on top of active surface of the solar panels, according to Eq. 3,

$$Q_e = \sum G_i \cdot \Delta t_i \cdot S \qquad 3$$

where S (m^2) is the solar receiver surface, G_i (W.m^{-2}) the global irradiation registered within Δt_i (s) period of time.

The calculated value of Q_e corresponding to the first treated batch was about 52 kWh. Assuming that heat losses and thermal inertia of the tank are negligible, the thermal efficiency of the whole system was estimated to around 0.7. This value is in agreement with the use of flat collector thermal panels at working temperature within the range from ambient to few tens of Celsius degrees.

As PS oxidant is injected after 65 °C has been reached, up to 95 % pollutants removal rate was achieved right away after 1.5 h of reaction (**Fig. 9**). However, one can observe that more than 60 % global removal rate (regardless individual pollutant) was rapidly achieved within the first 15 min of treatment, indicating relative high rate of degradation oxidation reactions. As expected from preliminary studies, the degradation of pollutants is very effective should the required condition of temperature is met.

If persulfate was injected below 65 °C, preliminary experiment (results not presented) showed an important activity regarding oxidant consumption as WW bulk temperature increased slowly under solar streaming heating. By the meantime, very little activity and low rate degradation of pollutant was obtained. This result points out the necessity of injecting the oxidant at the right temperature to guarantee a minimum rate of sulfate radicals production. ~~The issue will be discussed with more details on a future paper.~~

After completion of treatment on Day 2, solar energy accumulation kept going on until the end of the day, together with elevation of the effluent temperature (Fig. 8).

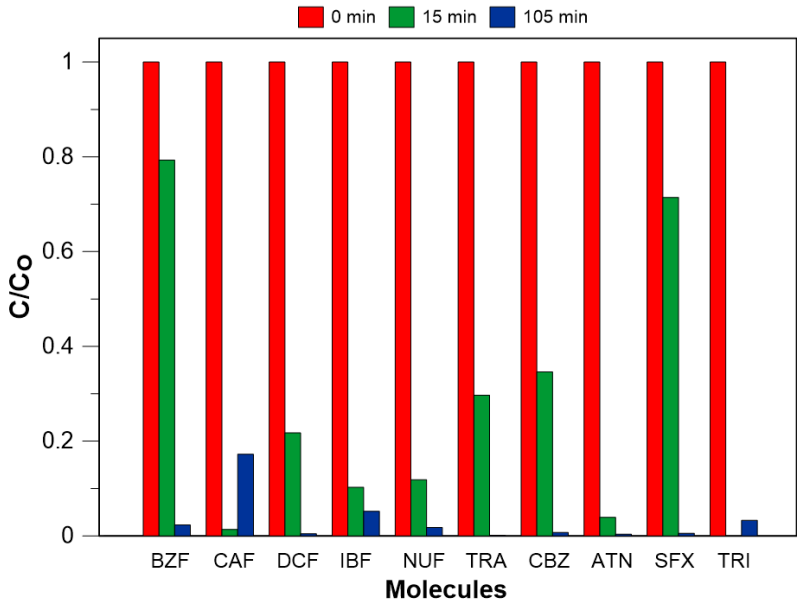

Fig. 9. Pollutants kinetic profile on Day 2 (Fig. 8)

On Day 3, heat energy recovered from the WW effluent treated the day before was used to raise temperature of new polluted WW batch entering in from 25 °C of ambient to about 50 °C (Fig. 10). This simple heat exchange operation took about 4 h to bring a preheated new polluted WW batch at the level of the treatment tank. Afterward, few hours of solar irradiation were needed to reach 65 °C and achieved degradation of pollutants on a second new WW batch in the row, as soon as PS oxidant was injected in.

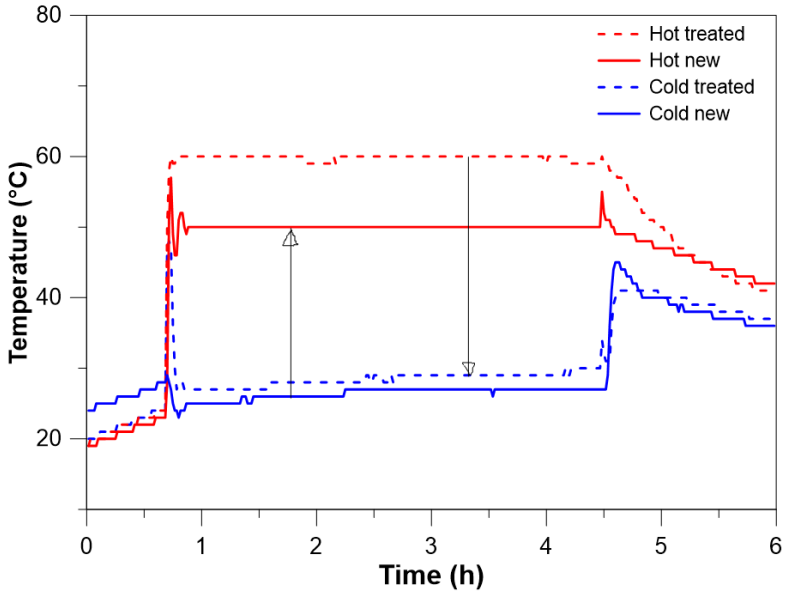

Fig. 10. Temperature profile over the heat exchange system with volumetric flow rates of the fluids equal to 200 $L.h^{-1}$.

Interestingly, thanks to the heat exchange system, it then takes less time (about 6 h including heat exchange time) under solar irradiation to reach 65 °C target temperature, as compared to the time needed for the first batch (Fig. 8). Within the two hours that immediately follow, pollutant degradation takes place (Fig. 11.a) after PS oxidant has been injected. A third and fourth additional batch treatment were achieved after repeating the same transfer-heat exchange procedure on day 4 and day 5 (Fig. 11.b).

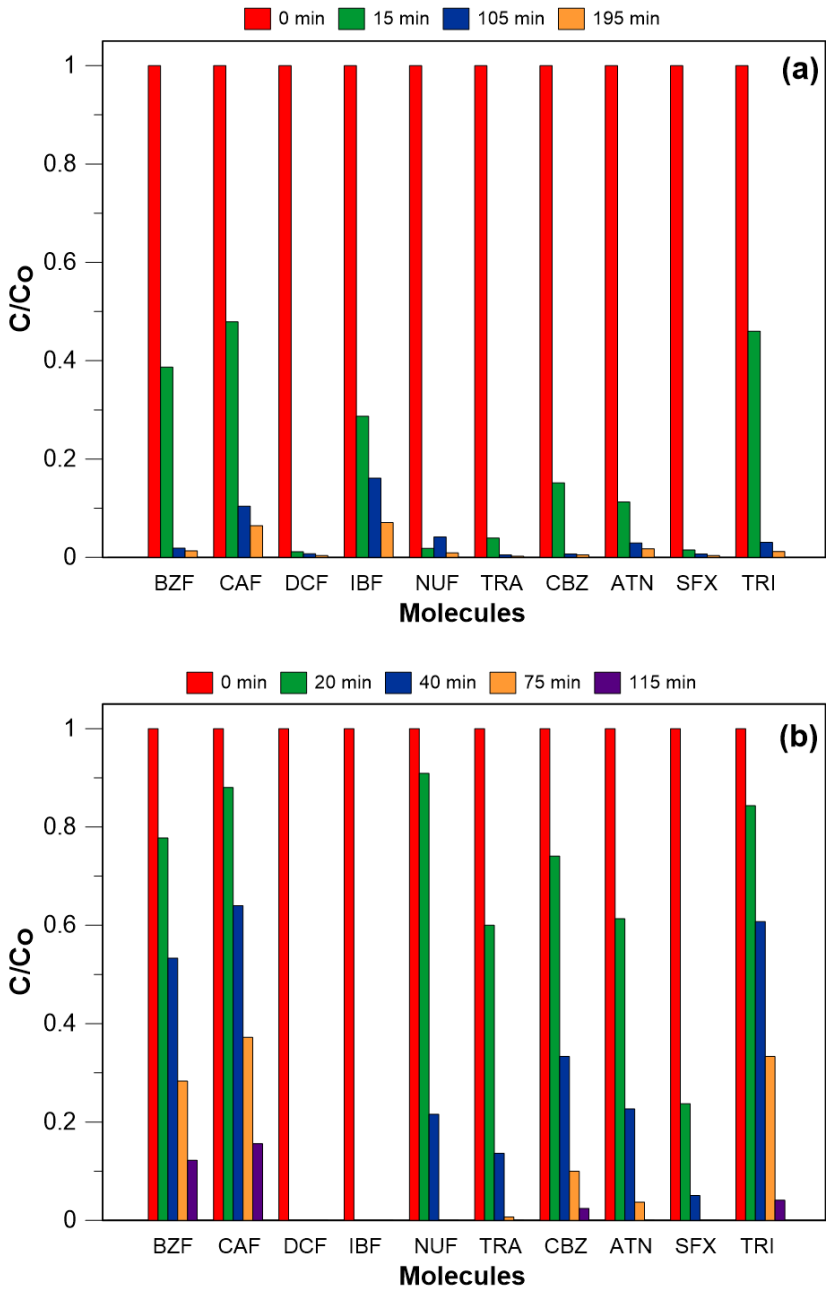

Fig. 11. Pollutants kinetic profiles on (a) Day 3 and (b) Day 5 (Fig. 8)

For day 3 and 4 (Fig. 8), the mean value of the amount of solar energy collected to drive pollutant degradation (i.e. periods between time of injection on day *n-1* and the injection time on day *n*) is about 38 kWh, corresponding to 47 Wh/L. This value is 25% smaller than solar energy needed on a process without heat energy recovery (52 kWh required for the first treated batch). This is a promising finding of what stands as the energy optimization approach. However, more efficiency is likely to be achieved regarding energy balance, together with some improvements over the heat management system. Some of these improvements deal with a more suitable sizing of heat exchanger and minimization of energy losses due to inertia of

materials the effluent is in contact with, and, more basically, an improvement of the system compactness.

.

On the other hand, it's worth mentioning that the heat management system copes with the discontinuous feature of sun light energy as applicable on Day 5 (Fig. 8**)**. Despite a poor solar irradiation conditions of this day, energy collected by the system was sufficient to raise WW effluent up to the target temperature, and to treat a fourth batch of 800 L WW (Fig. 11.b). More than 80% of pollutant global charge is removed after PS oxidant injection.

4. Conclusion

Persulfate thermal activation can be effective in removing emerging contaminants in water via advanced oxidation reactions. In this paper, persulfate is thermally activated on a solar pilot to drive degradation of ten target pollutants typically found in wastewater streams. Preliminary studies were first carried out prior to outdoor experimentations on real solar pilot equipment of 1000 L capacity. Indoor preliminary experiments highlighted how increasing temperature and oxidant concentration has a positive effect~~impact~~ on pollutants degradations rate. A slight variation of degradation rate can be observed from one individual pollutant to another. However, out of the ten, only Cafeine and Tramadol is still found in very few residual amount in the treated solution after 2 hours of treatment (at 70°C with 200 µM PS concentration). Regarding pilot scale equipment, experiments were carried out on batches of several hundreds of liters to make a proof of concept demonstration under real solar irradiation. The degradation of pollutants is effective o~~ver~~ a bulk treated volume (800 L) heated under solar irradiation above the 65 °C target temperature. Similarly to the small scale laboratory tests, around two hours were needed to achieve high removal rate of the 10 micropollutants cocktail within a real waste water effluent. The heat recovery system on the pilot definitely plays a key role to improve the energy balance and a smart use of solar energy collected on the top of basic solar panels. Since the heat energy collected can be stored over time, it allows an optimal running of the system, in particular during days with less fair weather episodes. The next critical step will be the optimization of energy balance to make the process competitive for the treatment of micropollutants in WW, with low investment on the extent of solar panels. Anyway, the general principle of a solar thermal activation of persulfate is experimentally demonstrated on a pilot scale set up.

Acknowledgements. The results published in this research paper are part of the findings of the INTERREG FEDER project called 4Kets4Reuse. The authors are thankful to the European project funding.

References

Aguas, Y., Hincapie, M., Martínez-Piernas, A.B., Agüera, A., Fernández-Ibáñez, P., Nahim-Granados, S., Polo-López, M.I., 2019. Reclamation of Real Urban Wastewater Using Solar Advanced Oxidation Processes: An Assessment of Microbial Pathogens and 74 Organic Microcontaminants Uptake in Lettuce and Radish. Environ. Sci. Technol. 53, 9705–9714.

Amor, C., Rodríguez-Chueca, J., Fernandes, J.L., Domínguez, J.R., Lucas, M.S., Peres, J.A., 2019. Winery wastewater treatment by sulphate radical based-advanced oxidation processes (SR-AOP): Thermally vs UV-assisted persulphate activation. Process Saf. Environ. Prot. 122, 94–101.

Brienza, M., Chiron, S., 2017. Enantioselective reductive transformation of climbazole: A concept towards quantitative biodegradation assessment in anaerobic biological treatment processes. Water Res. 116, 203–210.

Brienza, M., Mahdi Ahmed, M., Escande, A., Plantard, G., Scrano, L., Chiron, S., A. Bufo, S., Goetz, V., 2014. Relevance of a photo-Fenton like technology based on peroxymonosulphate for 17β-estradiol removal from wastewater. Chem. Eng. J. 257, 191–199.

Brienza, M., Mahdi Ahmed, M., Escande, A., Plantard, G., Scrano, L., Chiron, S., Bufo, S.A., Goetz, V., 2016. Use of solar advanced oxidation processes for wastewater treatment: Follow-up on degradation products, acute toxicity, genotoxicity and estrogenicity. Chemosphere 148, 473–480.

Cai, J., Zhou, M., Yang, W., Pan, Y., Lu, X., Serrano, K.G., 2018. Degradation and mechanism of 2,4-dichlorophenoxyacetic acid (2,4-D) by thermally activated persulfate oxidation. Chemosphere 212, 784–793.

Clarizia, L., Russo, D., Di Somma, I., Marotta, R., Andreozzi, R., 2017. Homogeneous photo-Fenton processes at near neutral pH: A review. Appl. Catal. B Environ. 209, 358–371.

Cuervo Lumbaque, E., Salmoria Araújo, D., Moreira Klein, T., Lopes Tiburtius, E.R., Argüello, J., Sirtori, C., 2019. Solar photo-Fenton-like process at neutral pH: Fe(III)-EDDS complex formation and optimization of experimental conditions for degradation of pharmaceuticals. Catal. Today, SI: SPEA10 328, 259–266.

Deng, J., Shao, Y., Gao, N., Deng, Y., Zhou, S., Hu, X., 2013. Thermally activated persulfate (TAP) oxidation of antiepileptic drug carbamazepine in water. Chem. Eng. J. 228, 765–771.

Devi, P., Das, U., Dalai, A.K., 2016. In-situ chemical oxidation: Principle and applications of peroxide and persulfate treatments in wastewater systems. Sci. Total Environ. 571, 643–657.

Durán, A., Monteagudo, J.M., San Martín, I., Aguirre, M., 2010. Decontamination of industrial cyanide-containing water in a solar CPC pilot plant. Sol. Energy 84, 1193–1200. https://doi.org/10.1016/j.solener.2010.03.025

Fan, Y., Ji, Y., Kong, D., Lu, J., Zhou, Q., 2015. Kinetic and mechanistic investigations of the degradation of sulfamethazine in heat-activated persulfate oxidation process. J. Hazard. Mater. 300, 39–47.

Faraldos, M., Bahamonde, A., 2017. Environmental applications of titania-graphene photocatalysts. Catal. Today, Women in Catalysis 285, 13–28.

Ferro, G., Polo-López, M.I., Martínez-Piernas, A.B., Fernández-Ibáñez, P., Agüera, A., Rizzo, L., 2015. Cross-Contamination of Residual Emerging Contaminants and Antibiotic Resistant Bacteria in Lettuce Crops and Soil Irrigated with Wastewater Treated by Sunlight/H2O2. Environ. Sci. Technol. 49, 11096–11104.

Ghauch, A., Tuqan, A.M., Kibbi, N., 2015. Naproxen abatement by thermally activated persulfate in aqueous systems. Chem. Eng. J. 279, 861–873.

Ghauch, A., Tuqan, A.M., Kibbi, N., 2012. Ibuprofen removal by heated persulfate in aqueous solution: A kinetics study. Chem. Eng. J. 197, 483–492.

Heizer, W.D., Sandler, R.S., Seal, E., Murray, S.C., Busby, M.G., Schliebe, B.G., Pusek, S.N., 1997. Intestinal Effects of Sulfate in Drinking Water on Normal Human Subjects. Dig. Dis. Sci. 42, 1055–1061.

Ike, I.A., Linden, K.G., Orbell, J.D., Duke, M., 2018. Critical review of the science and sustainability of persulphate advanced oxidation processes. Chem. Eng. J. 338, 651–669.

Ji, Y., Dong, C., Kong, D., Lu, J., Zhou, Q., 2015. Heat-activated persulfate oxidation of atrazine: Implications for remediation of groundwater contaminated by herbicides. Chem. Eng. J. 263, 45–54.

Johnson, R.L., Tratnyek, P.G., Johnson, R.O., 2008. Persulfate Persistence under Thermal Activation Conditions. Environ. Sci. Technol. 42, 9350–9356.

Liang, C., Huang, C.-F., Mohanty, N., Kurakalva, R.M., 2008. A rapid spectrophotometric determination of persulfate anion in ISCO. Chemosphere 73, 1540–1543.

Liu, X., Zhou, Y., Zhang, J., Luo, L., Yang, Y., Huang, H., Peng, H., Tang, L., Mu, Y., 2018. Insight into electro-Fenton and photo-Fenton for the degradation of antibiotics: Mechanism study and research gaps. Chem. Eng. J. 347, 379–397.

Malato, S., Maldonado, M.I., Fernández-Ibáñez, P., Oller, I., Polo, I., Sánchez-Moreno, R., 2016. Decontamination and disinfection of water by solar photocatalysis: The pilot plants of the Plataforma Solar de Almeria. Mater. Sci. Semicond. Process., Materials for applications in water treatment and water splitting 42, 15–23.

Marjanovic, M., Giannakis, S., Grandjean, D., de Alencastro, L.F., Pulgarin, C., 2018. Effect of μM Fe addition, mild heat and solar UV on sulfate radical-mediated inactivation of bacteria, viruses, and micropollutant degradation in water. Water Res. 140, 220–231.

Matzek, L.W., Carter, K.E., 2016. Activated persulfate for organic chemical degradation: A review. Chemosphere 151, 178–188.

Miralles-Cuevas, S., Oller, I., Ruíz-Delgado, A., Cabrera-Reina, A., Cornejo-Ponce, L., Malato, S., 2018. EDDS as complexing agent for enhancing solar advanced oxidation processes in natural water: Effect of iron species and different oxidants. J. Hazard. Mater. https://doi.org/10.1016/j.jhazmat.2018.03.018

Oh, W.-D., Dong, Z., Lim, T.-T., 2016. Generation of sulfate radical through heterogeneous catalysis for organic contaminants removal: Current development, challenges and prospects. Appl. Catal. B Environ. 194, 169–201.

Olmez-Hanci, T., Arslan-Alaton, I., Genc, B., 2013. Bisphenol A treatment by the hot persulfate process: Oxidation products and acute toxicity. J. Hazard. Mater. 263, 283–290.

Shawaqfeh, A.T., Al Momani, F.A., 2010. Photocatalytic treatment of water soluble pesticide by advanced oxidation technologies using UV light and solar energy. Sol. Energy 84, 1157–1165. https://doi.org/10.1016/j.solener.2010.03.020

Soriano-Molina, P., García Sánchez, J.L., Alfano, O.M., Conte, L.O., Malato, S., Sánchez Pérez, J.A., 2018. Mechanistic modeling of solar photo-Fenton process with Fe3+-EDDS at neutral pH. Appl. Catal. B Environ. 233, 234–242.

Strazzabosco, A., Kenway, S.J., Lant, P.A., 2019. Solar PV adoption in wastewater treatment plants: A review of practice in California. J. Environ. Manage. 248, 109337.

Vilar, V.J.P., Pinho, L.X., Pintor, A.M.A., Boaventura, R.A.R., 2011. Treatment of textile wastewaters by solar-driven advanced oxidation processes. Sol. Energy 85, 1927–1934. https://doi.org/10.1016/j.solener.2011.04.033

Wu, Y., Brigante, M., Dong, W., de Sainte-Claire, P., Mailhot, G., 2014. Toward a Better Understanding of Fe(III)–EDDS Photochemistry: Theoretical Stability Calculation and Experimental Investigation of 4-tert-Butylphenol Degradation. J. Phys. Chem. A 118, 396–403.

Yang, J.-F., Yang, L.-M., Zhang, S.-B., Ou, L.-H., Liu, C.-B., Zheng, L.-Y., Yang, Y.-F., Ying, G.-G., Luo, S.-L., 2017. Degradation of azole fungicide fluconazole in aqueous solution by thermally activated persulfate. Chem. Eng. J. 321, 113–122.

Zhao, L., Yang, S., Wang, L., Shi, C., Huo, M., Li, Y., 2015. Rapid and simple spectrophotometric determination of persulfate in water by microwave assisted decolorization of Methylene Blue. J. Environ. Sci. 31, 235–239.